

Short communication

Composite bounds on the elastic modulus of bone

Michelle L. Oyen^{a,b,*}, Virginia L. Ferguson^{b,c}, Amanpreet K. Bembey^b,
Andrew J. Bushby^b, Alan Boyde^d^a*Department of Engineering, University of Cambridge, Trumpington Street, Cambridge CB2 1PZ, UK*^b*Department of Materials, Queen Mary, University of London, London E1 4NS, UK*^c*Department of Mechanical Engineering, University of Colorado, Boulder, CO 80309, USA*^d*Oral Growth and Development, Queen Mary, University of London, London E1 1BB, UK*

Accepted 14 May 2008

Abstract

Advances in diagnosis and treatment of some bone disorders can be made by understanding the linkage between mineral content and mechanical function. Bone is approximately half by volume a hydrated protein network, and the remainder is a biomineral analogue of hydroxyapatite. In the current work, paired measurements of mechanical properties, using nanoindentation, and of bone mineral volume fraction, computed from quantitative back-scattered electron imaging, were made on six different types of normal and outlier bone samples. Local elastic modulus was plotted against mineral fraction and compared with predictions of engineering bounds for a two-phase composite material. Experimental data spanning the composite bounds showed no one-to-one relationship between mechanical stiffness and bone composition, excluding the possibility of any single, simple composites model for bone at nanometer length-scales. © 2008 Elsevier Ltd. All rights reserved.

Keywords: Bone; Nanoindentation; Composite bounds; Elastic modulus; Mineral volume fraction

1. Introduction

The mechanical performance of bone depends on its composition and particularly its mineral density. Bone and other biological tissues are similar to engineered composite materials, with combinations of properties not found in any monolithic material. As such, bone has been considered in an engineering composite materials framework since pioneering work in the 1960s and 1970s (Currey, 1964; Katz, 1971). Recent research has sought an expression for the relationship between mineral composition and mechanical stiffness (i.e. elastic modulus) of bone tissue, in many cases using a composite mechanics approach (Hellmich and Ulm, 2002).

In composite mechanics, bounds on the elastic modulus of the composite are computed from the elastic moduli of

the component materials. The weighting depends on the amounts and physical organization of the components, including the phase volume fractions and the size, shape, distribution and orientation of the components. For aligned fiber composites, the Voigt–Reuss bounds (Herakovich, 1997) give upper and lower modulus bounds in directions parallel and perpendicular to the fiber directions, respectively. For spherical particle composites (as an exact solution from the Hashin–Shtrikman (H–S) bounds (Hashin and Shtrikman, 1963)), the lower H–S bound physically represents stiff particles embedded in a continuous compliant phase and the upper H–S bound represents compliant particles embedded in a continuous stiff phase (Fig. 1).

The advent of nanoindentation testing has allowed local mechanical properties measurements at length-scales comparable to the most fundamental structural length-scales in bone hierarchy: nanometer-scale collagen molecules and mineral dimensions. In this paper, site-matched measurements are made of the bone elastic modulus and mineral volume fraction. Tests were conducted on each of the six

*Corresponding author at: Department of Engineering, University of Cambridge, Trumpington Street, Cambridge CB2 1PZ, UK.

Tel.: +44 1223 332 680; fax: +44 1223 332 662.

E-mail address: mlo29@cam.ac.uk (M.L. Oyen).

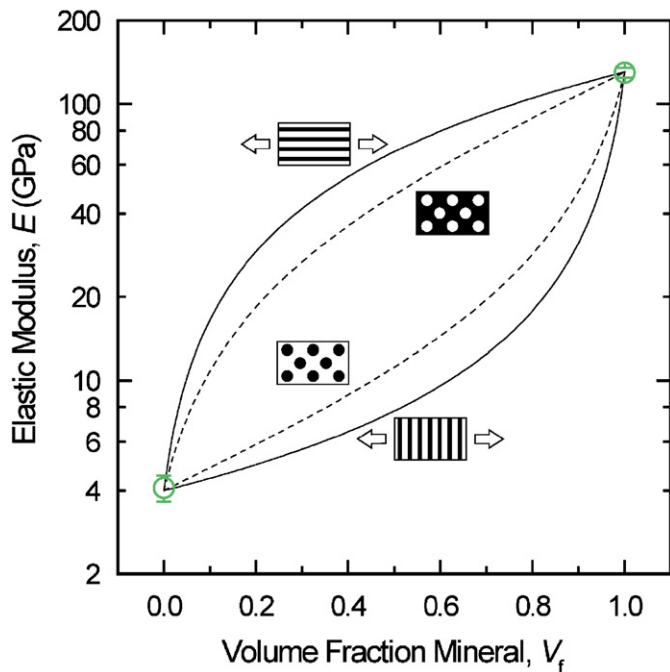


Fig. 1. Composite elastic modulus bounds for various structures, expressed in terms of the volume fraction of the stiff phase, together with illustrations of the corresponding physical structures (black represents the stiff phase). The solid lines are Voigt–Reuss composite bounds for a stiff fiber reinforcing phase, and dotted lines represent the Hashin–Shtrikman bounds for particle composites.

different bone types and compared with composite bounds for a two-phase material to elucidate the relationship between bone stiffness and mineral content and to assess the predictability of one property from the other.

2. Methods

Human bone samples were isolated from osteomalacic iliac crest (Schnitzler et al., 1994), cadaveric mandible (Kingsmill and Boyde, 1998), normal postmortem femoral head (Ferguson et al., 2003), and cadaveric incus (Macconnachie et al., 1985); whale specimens were from baleen (fin) whale otic bone and dense-beaked whale rostrum (Currey, 2002). All samples were dehydrated in ethanol and embedded in polymethyl methacrylate (PMMA), diamond micro-milled to an optically flat finish and carbon coated for examination in the scanning electron microscope (SEM).

Site-matched measurements of the elastic modulus and physical density were obtained at a typical spacing of 15 or 20 μm in grid arrays covering approximately one-quarter of a square millimeter (Bushby et al., 2004; Ferguson et al., 2003). Elastic modulus values were determined by nanoindentation (Bushby et al., 2004) (UMIS 2000, CSIRO, Australia) using a spherical-tipped indenter (nominal radius of 5 μm). The partial-unloading method (Field and Swain, 1993) was used to determine indentation elastic modulus. A value for Poisson's ratio of 0.3 was used in the calculation of Young's modulus for all bone tissues tested (Zysset et al., 1999). Indentation data were collected from sample surfaces in various orientations relative to the tissue orientation (along longitudinal and transverse planes).

Indented regions of each sample were imaged using quantitative back-scattered electron (qBSE) imaging in an automated digital SEM (Zeiss DSM962 with Kontron IBAS external computer control), as described previously (Ferguson et al., 2003). The qBSE gray levels were obtained for halogenated dimethacrylate standards (Howell and Boyde, 1998a; Howell

et al., 1998b) and a nonlinear calibration curve established to convert bone qBSE gray level values to equivalent mineral volume fraction (V_f).

The modulus values for the extremes of mineral volume fraction ($V_f = 0$ or 1) were also obtained by nanoindentation experiments ($E = 4.1 \pm 0.4$ GPa for unmineralized osteoid embedded in PMMA and $E = 129.5 \pm 5.2$ GPa for mineralogical apatite), as are shown by the endpoints in Fig. 1. Composite bounds (Herakovich, 1997; Hashin and Shtrikman, 1963) were computed from these extremal modulus values assuming a Poisson's ratio of 0.3 for both phases.

3. Results

Matched elastic modulus–mineral volume fraction (E – V_f) points are plotted in Fig. 2 from a total of $n = 3710$ individual measurements on human (femur, mandible, incus, and iliac crest) and baleen (fin) and toothed (dense beaked) whale bone. Over the range of bone samples studied, the mineral content varied from 0% to 80%, and the elastic modulus from the baseline (osteoid in PMMA) modulus of 4 GPa to nearly 70 GPa in the whale bones. At any one mineral concentration, a large range of modulus values were found, and any one modulus value were found a range of compositional values. Overall, the lowest modulus values were not less than the lower H–S bound and the greatest modulus values approached the upper H–S bound. The majority of the experimental data in Fig. 2(a) lie in the intermediate region. Fig. 2(b) shows the median modulus as a function of median mineral fraction for each of the six bone types.

4. Discussion

This study demonstrates a wide range of composition–stiffness combinations that can result in a material that is nonetheless in all cases recognized as bone. There is a general trend towards increased elastic modulus with increased mineral fraction in the whole data set, but at any single value of one variable (modulus or mineral volume fraction) the complementary parameter varies widely. Nanoscale variations in composition and structure are known to exist within bone. It has been hypothesized (Tai et al., 2007) that these variations add functionality at the bone tissue level including local signalling of strain to osteocytes, and perhaps contributing a toughening mechanism compared with a homogeneous material.

Two potentially confounding effects were not considered in the current study. The bone samples were embedded in PMMA, and were tested effectively dry such that the effects of hydration state (Bembey et al., 2006a) or time-dependent creep flow (Cowin, 1999) were not considered. Emphasis on the current study was on the mineral phase, which has an elastic modulus value more than an order of magnitude greater than the protein phase. In addition, the effect of potential anisotropy was not explicitly considered. The bone samples were tested in indentation, which causes a slight diminution of anisotropy, since the indentation test samples several orientations at once (Swadener et al., 2001). The maximum differences in elastic modulus with

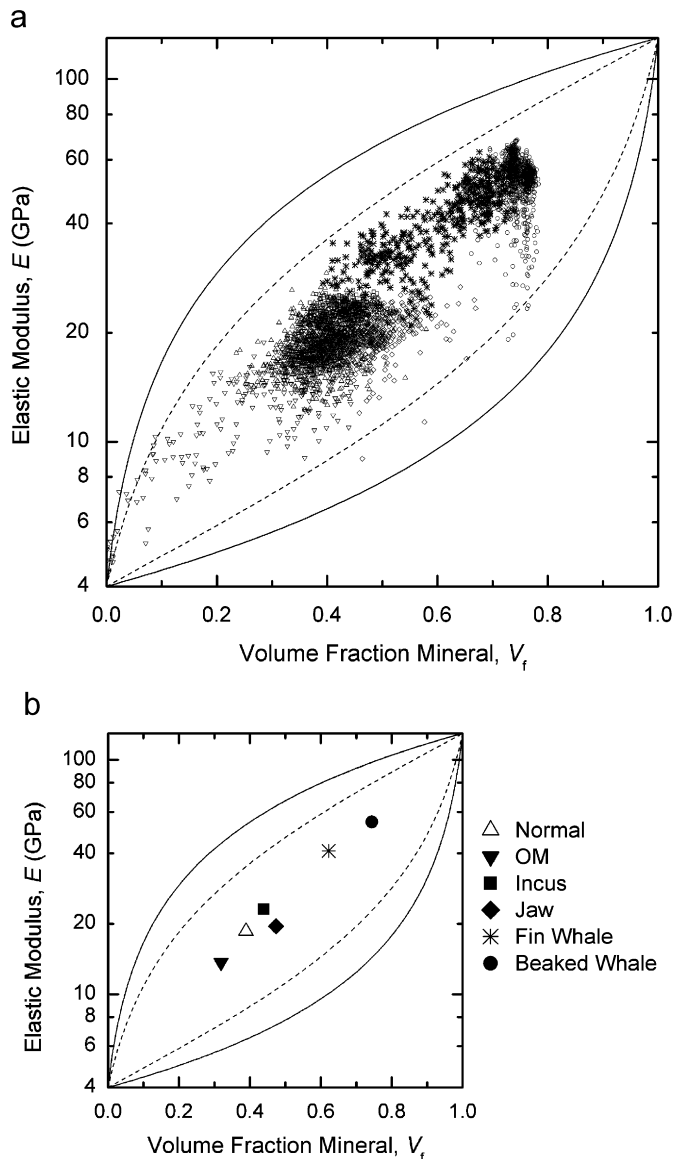


Fig. 2. (a) Experimental data for the elastic modulus (E) versus mineral concentration (volume fraction, V_f) of PMMA-embedded bone samples: human femoral head; human osteomalacic iliac crest (OM); human incus; human mandible; fin whale otic bone; dense beaked whale rostrum. The solid lines are Voigt–Reuss bounds and dashed lines are Hashin–Shtrikman bounds. (b) Median elastic modulus (E) versus median mineral volume fraction, V_f , for the data shown in part (a) and with the same legends.

bone direction due to anisotropy (Swadener et al., 2001) are significantly smaller than the large differences in elastic modulus observed over a range of modulus values in the current study. Similarly, the variations observed experimentally were substantially greater than established uncertainties in the measurement techniques utilized herein. The measurement variation observed in calibration and standard measurements for both elastic modulus (Bembey et al., 2006b) and qBSE data (Angker et al., 2004) is approximately 4%. Thus, although individual points on the plot in Fig. 2(a) could be shifted slightly from their locations on the graph, the overall observed variability is large and due

to the material itself. The placement of an indentation grid within a representative region of tissue enabled a statistical sampling of closely spaced points (Constantinides et al., 2006), and did not target the analysis with specific material characteristics *a priori*.

There are biological explanations for some of the wide range in observed behavior. In normal bone, the volume fraction of mineral is limited to a maximum of approximately 50% V_f by the fact that the rest of the space is occupied by collagen, other organic matrix components and water. In osteomalacic bone, the protein matrix is formed (osteoid), but is patchily and poorly mineralized, resulting in low values for both modulus and mineral fraction. Whale bones demonstrate both increased mineral content and mechanical stiffness compared with normal bone. Mineral volume fractions in these bone samples exceed values possible without any degradation of the organic matrix. That matrix reduction has likely occurred in such cases is supported by transmission electron microscopy observations (Zylberberg et al., 1998).

The composites framework provides additional information in comparing bone types by paired median E – V_f measurements (Fig. 2(b)), instead of comparing each parameter individually. There is increased mineral content in both the jaw and incus data compared with normal bone, but only the incus demonstrates increased mechanical stiffness. It is expected that this approach for comparison of data would be useful in clinical studies of bone, such as osteoporosis drug studies.

The dispersion of data observed in the current study is critical in considering recent efforts to model bone as a composite material. Katz (1971) noted that the increase in bone modulus at fixed composition could not be predicted by composite bounds, since data spanned the bounds at fixed composition. In the current study, this result is expanded to demonstrate that the local modulus-mineral points essentially fill the space demarked by the H–S bounds. Therefore, no single relationship can exist for prediction of modulus from composition and, conversely, there is no means to predict mineral concentration solely from elastic modulus values. Simple models of bone as a composite, assuming uniform structures and allowing for direct one-to-one E – V_f relationships, are thus inconsistent with the observed experimental data (Fig. 2(a)).

A further implication of this finding is that a range of local structural arrangements of mineral and organic phases must exist in bone at fixed composition to give rise to different modulus values. The difference between the composite bounds is greatest at 50% mineral volume fraction, the approximate composition of normal bone. This parallels the peak in entropy observed, in which the maximum number of possible arrangements of the two phases exists (Gaskell, 1981). Advanced models are needed, based on statistical processes, to predict distributions of modulus values from composition. One mechanism to produce bone-like structures (and structure variations) in biomimetic or tissue engineering applications may be to

focus on biomimetic processes (Chang et al., 2003), which may result in engineered structures that are optimized for fracture resistance.

Conflict of interest statement

The authors declare no conflict of interest associated with this work.

Acknowledgments

The authors thank Maureen Arora for technical assistance. AB was supported by the Veterinary Advisory Committee of the Horserace Betting Levy Board. The facility for the determination of bone mineralisation density at the microscopic scale was funded by the Medical Research Council (MRC) of UK. MLO thanks C.-C. Ko for helpful discussions on this topic. Fin whale otic and dense-beaked whale rostrum bone samples were the kind gift of Prof. John Currey, York.

References

- Angker, L., Nockolds, C., Swain, M.V., Kilpatrick, N., 2004. Quantitative analysis of the mineral content of sound and carious primary dentine using BSE imaging. *Archives of Oral Biology* 49, 99–107.
- Bembey, A.K., Bushby, A.J., Boyde, A., Ferguson, V.L., Oyen, M.L., 2006a. Hydration effects on bone mechanical properties. *Journal of Materials Research* 21, 1962–1968.
- Bembey, A.K., Oyen, M.L., Bushby, A.J., Boyde, A., 2006b. Viscoelastic properties of bone as a function of hydration state determined by nanoindentation. *Philosophical Magazine* 86, 5691–5703.
- Bushby, A.J., Ferguson, V.L., Boyde, A., 2004. Nanoindentation of bone: comparison of specimens in liquid and embedded in polymethylmethacrylate. *Journal of Materials Research* 19, 249–259.
- Chang, M.C., Ko, C.C., Douglas, W.H., 2003. Preparation of hydroxyapatite–gelatin nanocomposite. *Biomaterials* 24, 2853–2862.
- Constantinides, G., Ravi Chandran, K.S., Ulm, F.-J., Van Vliet, K.J., 2006. Grid indentation analysis of composite microstructure and mechanics: principles and validation. *Materials Science and Engineering A* 430, 189–202.
- Cowin, S.C., 1999. Bone poroelasticity. *Journal of Biomechanics* 32, 217–238.
- Currey, J.D., 1964. Three analogies to explain the mechanical properties of bone. *Biorheology* 2, 1–10.
- Currey, J.D., 2002. *Bones. Structure and Mechanics*. Princeton University Press, Princeton, NJ, USA.
- Ferguson, V.L., Bushby, A.J., Boyde, A., 2003. Nanomechanical properties and mineral concentration in articular calcified cartilage and subchondral bone. *Journal of Anatomy* 203, 191–202.
- Field, J.S., Swain, M.V., 1993. A simple predictive model for spherical indentation. *Journal of Materials Research* 8, 297–306.
- Gaskell, D.R., 1981. *Introduction to Metallurgical Thermodynamics*, second ed. Hemisphere Publishing Corporation (Taylor and Francis), New York.
- Hashin, Z., Shtrikman, S., 1963. *Journal of the Mechanics and Physics of Solids* 11, 127–140.
- Hellmich, C., Ulm, F.-J., 2002. Are mineralized tissues open crystal foams reinforced by crosslinked collagen?—Some energy arguments. *Journal of Biomechanics* 35, 1199–1212.
- Herakovich, C.T., 1997. *Mechanics of Fibrous Composites*. Wiley, New York, USA.
- Howell, P.G.T., Boyde, A., 1998a. Monte Carlo simulation of electron backscattering from compounds with low mean atomic number. *Scanning* 20, 45–49.
- Howell, P.G.T., Davy, K.M.W., Boyde, A., 1998b. Mean atomic number and backscattered electron coefficient calculations for some materials with low mean atomic number. *Scanning* 20, 35–40.
- Katz, J.L., 1971. Hard tissue as a composite material. I. Bounds on the elastic behavior. *Journal of Biomechanics* 4, 455–473.
- Kingsmill, V.J., Boyde, A., 1998. Mineralisation density of human mandibular bone: quantitative backscattered electron image analysis. *Journal of Anatomy* 192, 245–256.
- Maconnachie, E., Reid, S.A., Jones, S.J., Lewis, A., Frootko, N., Boyde, A., 1985. SEM studies of auditory ossicles in man and rat. *Bone* 6, 404–405.
- Schnitzler, C.M., Pettifor, J.M., Patel, D., Mesquita, J.M., Moodley, G.P., Zachen, D., 1994. Metabolic bone disease in black teenagers with genu valgum or varum without radiologic rickets: a bone histomorphometric study. *Journal of Bone and Mineral Research* 9, 479–486.
- Swadener, J.G., Rho, J.-Y., Pharr, G.M., 2001. Effects of anisotropy on elastic moduli measured by nanoindentation in human tibial cortical bone. *Journal of Biomedical Materials Research* 57, 108–112.
- Tai, K., Dao, M., Suresh, S., Palazoglu, A., Ortiz, C., 2007. Nanoscale heterogeneity promotes energy dissipation in bone. *Nature Materials* 6, 454–462.
- Zylberberg, L., Traub, W., de Buffrenil, V., Allizard, F., Arad, T., Weiner, S., 1998. Rostrum of a toothed whale: ultrastructural study of a very dense bone. *Bone* 23, 241–247.
- Zysset, P.K., Guo, X.E., Hoffler, C.E., Moore, K.E., Goldstein, S.A., 1999. Elastic modulus and hardness of cortical and trabecular bone lamellae measured by nanoindentation in the human femur. *Journal of Biomechanics* 32, 1005–1012.